Journal of Molecular Catalysis A: Chemical 319 (2010) 71–77

Contents lists available at ScienceDirect

Journal of Molecular Catalysis A: Chemical

journal homepage: www.elsevier.com/locate/molcata

Preparation and catalytic properties of fine particles of Pt-Ge intermetallic compound formed inside the mesopores of MCM-41

Takayuki Komatsu[a,*], Kazunori Sou[a], Ken-ichi Ozawa[b]

[a] Department of Chemistry, Tokyo Institute of Technology, 2-12-1-E1-10 Ookayama, Meguro-ku, Tokyo 152-8550, Japan
[b] Department of Chemistry and Materials Science, Tokyo Institute of Technology, 2-12-1-E1-10 Ookayama, Meguro-ku, Tokyo 152-8550, Japan

ARTICLE INFO

Article history:
Received 2 September 2009
Received in revised form 3 December 2009
Accepted 4 December 2009
Available online 30 December 2009

Keywords:
Intermetallic compound
MCM-41
Nano particle
Platinum
Partial hydrogenation

ABSTRACT

Fine particles of Pt-Ge intermetallic compound were prepared by using mesoporous silica MCM-41 as a support and examined as a catalyst for H_2–D_2 equilibration and the hydrogenation of acetylene to clarify the catalytic properties of single-phase intermetallic compound with nano-order particle size. The mesopore structure of MCM-41 was not affected extensively by the introduction of Pt and Ge. Pt-Ge particles on MCM-41 gave very narrow particle-size distribution around 1.5 nm, suggesting the presence of Pt-Ge particles inside the mesopores of MCM-41, whereas those prepared on silica gel had the wide distribution of 1–6 nm. Though the Pt-Ge particles on MCM-41 were too small to identify their crystal phase by XRD, IR spectra of adsorbed CO indicated the presence of intermetallic phase, probably PtGe. Pt-Ge/MCM-41 showed lower catalytic activity than PtGe/SiO_2 for H_2–D_2 equilibration at 77 K and an induction period was observed for the former catalyst. The physically adsorbed hydrogen molecules may hinder the diffusion of HD through the mesopores. Pt-Ge/MCM-41 showed higher selectivity to ethylene than Pt/MCM-41 in the hydrogenation of acetylene, which again indicates the formation of PtGe intermetallic compound.

1. Introduction

Intermetallic compounds (IMCs) are the stoichiometric compounds between two or more metal elements. As compared with usual alloy, which is a solid solution having the same crystal structure as that of either component metal, various IMCs have their specific crystal structures different from those of their component metals. The specific crystal structure and the combination of two elements sometimes give IMCs unique bulk properties, such as super conductivity, hydrogen storage ability, shape memory effect, etc. However, their catalytic properties, one of the important surface natures, have never been studied sufficiently. We have studied the catalytic properties of single-phase IMCs as compared with those of pure metals [1]. In the hydrogenation of acetylene, CoGe [2], Ni_3Sn and Ni_3Sn_2 [3] have higher selectivity to ethylene than Co and Ni. Recently, Studt et al. [4] explained the higher ethylene selectivity of NiZn than Ni by the change in heats of adsorption of hydrocarbons. Kovnir et al. [5] have reported that the high ethylene selectivity of PdGa is attributable to the isolation of surface Pd atoms by the formation of IMC with Ga. We have also reported that Pt_3Ge has higher selectivity to butenes than Pt in the hydrogenation of 1,3-butadiene [6]. Pt_3Ti shows higher activity than Pt for H_2–D_2 equilibration and the hydrogenation of ethylene [7]. $CoHf_2$ shows high activity and stability in the CO_2 reforming of methane [8]. Tsai et al. [9] reported the similarity in catalytic activity of PdZn to that of pure Cu in the steam reforming of methanol. However, these catalysts, which consisted of large grains of IMCs with the size of 10–50 μm, showed very low specific activity compared with supported metal catalysts containing nano-order metal particles.

To obtain highly active IMC catalysts, fine particles of IMC have to be prepared by fixing them on supports. Though many researchers have already reported that Pt-Sn IMC phases, for example, $PtSn_4$, PtSn, and Pt_2Sn [10], are present in supported Pt-Sn bimetallic catalysts used for petroleum reforming, metallic species are always the mixture of two or more metals, alloys, IMCs and even oxidized species. Therefore, the intrinsic catalytic properties of the specific Pt-Sn IMC have never been clarified. Some researchers have tried to prepare single-phase IMC particles on oxide supports. Iwasa et al. formed PdZn particles by reducing Pd/ZnO and found them active for the steam reforming of methanol [11]. Llorca et al. have prepared PtSn on SiO_2 by successive impregnation method [12]. We have prepared single-phase IMCs on the surface of silica gel [1]. First, each single-phase Ni-Sn IMC, Ni_3Sn, Ni_3Sn_2 and Ni_3Sn_4, was prepared by chemical vapor deposition (CVD) of $Sn(CH_3)_4$ onto Ni/SiO_2 under various conditions [13]. A similar CVD method has been applied to obtain RuTi/SiO_2 [14,15], Pd_3Bi/SiO_2 [16] and Pt_3Sn/H-SAPO-11 [17]. However, the particle size of these IMCs was not uniform. For the definite characterization and assignment of

* Corresponding author. Tel.: +81 3 5734 3532; fax: +81 3 5734 2758.
E-mail address: komatsu@chem.titech.ac.jp (T. Komatsu).

1381-1169/$ – see front matter © 2009 Elsevier B.V. All rights reserved.
doi:10.1016/j.molcata.2009.12.002

active sites, it will be better to obtain single-phase IMC particles with a uniform diameter. Moreover, the metal particles in uniform size would prove the relationship between the coordination number and catalytic properties, especially in so-called structure sensitive reactions. The role of corner and edge atoms has been reported for pure metal catalysts, such as Ni [18], Pt [19,20] and Rh [21].

We have previously reported [22] the preparation of Ni-Ge IMC particles inside the mesopores of MCM-41, which is a mesoporous silica having orderly hexagonal structure with a homogeneous pore diameter. Fine particles of single-phase Ni_3Ge were formed predominantly inside the mesopores through the successive loadings of Ni by template ion-exchange [23] and Ge by CVD. Ni_3Ge/MCM-41 thus prepared gave higher intrinsic activity than Ni/MCM-41 and Ni_3Ge/SiO_2 for H_2–D_2 equilibration and acetylene hydrogenation. In this study, we applied the above strategy to Pt-Ge IMCs because Pt is known to be extremely active compared with Ni for many reactions. The objectives of this study are to obtain uniform particles of Pt-Ge IMC inside the orderly mesopores of MCM-41 and clarify their catalytic properties.

2. Experimental

2.1. Catalyst preparation

MCM-41 mesoporous silica was synthesized hydrothermally [24]. The surfactant of cetyltrimethylammmonium bromide ($C_{16}H_{33}(CH_3)_3NBr$, 27 g) was dissolved into 270 g of pure water at 313 K. Coloidal silica (Nissan Chemical Ind., Snowtex 20, 159 g) and a 4.2% aqueous solution of sodium hydroxide (142 g) were dropped into the surfactant solution and the mixture was stirred for 1 h. The mixture was transferred into an autoclave and heated at 413 K for 48 h without stirring. The solid obtained was filtered, washed with pure water, dried at 353 K and calcined in air at 813 K for 10 h to obtain MCM-41.

Platinum was introduced by an ion-exchange technique [25] into MCM-41. MCM-41 (2.0 g) was put into an aqueous solution of ammonia (3×10^{-4} M) and the mixture was stirred for 1 h to transform SiOH into $SiONH_4$. The solid was filtered, washed with pure water and dried at 353 K to obtain NH_4^+-MCM-41. Tetraammineplatinum(II) acetate (N.E. Chemcat Corp., 0.047 g) was dissolved into 100 g of pure water and the solution was added to NH_4^+-MCM-41. After stirring it at 298 K for 1 h, the solid was filtered, washed with pure water, dried at 353 K and calcined in air at 473 K for 8 h to obtain PtO_x/MCM-41. The ammonium ion-exchange and Pt loading were repeated similarly onto PtO_x/MCM-41. Finally, Pt/MCM-41 was obtained through the reduction with flowing hydrogen (60 ml min^{-1}) at 473 K for 1 h.

Introduction of germanium was carried out by the CVD method in a similar manner to the preparation of Ni_3Ge/MCM-41 [22]. Pt/MCM-41 (0.40 g) was put into a quartz reactor (17 mm ID) and reduced in flowing hydrogen (60 ml min^{-1}) at 473 K for 1 h. After the temperature was set to 423 K, the vapor of $Ge(CH_3)_4$ saturated at 273 K in flowing hydrogen (30 ml min^{-1}) was introduced onto Pt/MCM-41 for 1 h as CVD treatment. The sample was further treated with flowing hydrogen (60 ml min^{-1}) at 873 K for 1 h to give Pt-Ge/MCM-41.

As a reference catalyst, Pt-Ge/SiO_2 was prepared stepwise through Pt/SiO_2 using silica gel (Caliact G6, Fuji Silysia). First, Pt(1 wt%)/SiO_2 was prepared by a usual pore-filling impregnation with an aqueous solution of tetraammineplatinum(II) acetate, followed by the calcination in air at 673 K and the reduction with flowing hydrogen at 773 K. Ge was then introduced by the CVD method in a similar manner to the Pt-Ge/MCM-41 preparation. The temperature of Pt/SiO_2 was set to 553 K during the CVD for 1 h.

2.2. Characterization

The structural information on MCM-41-supported catalysts was obtained by powder X-ray diffraction (XRD, Rigaku, RINT2400) and small angle X-ray scattering (SAXS, Rigaku, NANO-Viewer system) with Cu Kα X-ray. Nitrogen adsorption measurements were also conducted using Coulter SA-3100. The crystal structure of supported metal particles was examined also by XRD. TEM images were obtained by a Jeol JEM-2010F microscope. The bulk composition of prepared catalysts was determined by ICP (Rigaku, JY38) after dissolving samples with HF solution and aqua regia.

The amount of hydrogen adsorbed at 195 K was measured in a similar manner to the method reported by Freni et al. [26]. The sample (50 mg) was put into a quartz tube and reduced by flowing hydrogen (60 ml min^{-1}) for 1 h at 473 K for Pt/MCM-41, 773 K for Pt/SiO_2 and 873 K for Pt-Ge/MCM-41 and Pt-Ge/SiO_2. After hydrogen was purged by flowing argon for 10 min, the sample was cooled to 195 K. A pulse of H_2 (5.0×10^{-9} mol) diluted by argon was introduced with the outlet gas monitored by a thermal conductivity detector (TCD). The pulses were repeatedly introduced onto the sample to reach the adsorption equilibrium. Then, the sample was heated abruptly by a heating gun and the total amount of evolved H_2 was measured by the TCD. The amount of CO adsorbed at 298 K was measured by a usual pulse technique. Samples were pretreated by hydrogen at the same temperatures as those for the pretreatment for H_2 adsorption measurements. Then hydrogen was purged by flowing helium. A pulse of CO (5.0×10^{-9} mol) diluted by helium was introduced repeatedly at 298 K to reach the equilibrium to obtain the amount of irreversibly adsorbed CO.

IR spectra of adsorbed CO were measured with a JASCO FT/IR-430 spectrometer in its transmission mode. A self-supporting wafer (ca. 10 mg cm^{-2}) of catalyst was put in a quartz cell having CaF_2 windows. After the reduction in circulating hydrogen (15 kPa) at 673 K (473 K for Pt/MCM-41) for 1 h and the evacuation at the same temperature, the sample was cooled in vacuo to 298 K. CO (1.5 kPa) was introduced at 298 K and a spectrum was recorded with 0.5 cm^{-1} resolution and 50 scans. Spectra were further obtained after the evacuation at various temperatures.

2.3. Catalytic reactions

H_2–D_2 equilibration was carried out using a glass circulation system connected to a quadrupole mass-spectrometer (Canon Anelva, M-101QA-TDM). Before each reaction, 20 mg of catalyst was reduced with 15 kPa of circulating H_2 for 1 h at 473 K for Pt/MCM-41, 773 K for Pt/SiO_2 and 873 K for Pt-Ge/MCM-41 and PtGe/SiO_2, followed by the evacuation at the reduction temperature. A mixture of H_2 (6.7 kPa) and D_2 (99 atom%, 6.7 kPa) was circulated through the catalyst at 77 K. The extent of the equilibration reaction was monitored by the change in the fraction of HD in hydrogen, $HD/(H_2 + HD + D_2)$.

The hydrogenation of acetylene was carried out using a continuous flow reaction system under atmospheric pressure. The catalyst (20 mg) was placed in a tubular quartz reactor of 17 mm ID. Prior to the catalytic run, the catalyst was reduced with flowing hydrogen for 1 h at the same temperatures as those in H_2–D_2 equilibration. The reaction was started at 473 or 573 K by supplying a reactant gas composed of C_2H_2 (14 kPa), H_2 (29 kPa) and He (balance) with a total flow rate of 28 ml min^{-1}. Gaseous products were analyzed by using an FID gas chromatograph (Shimadzu, GC-14B) with a column of CP8567 (Varian). The selectivity to ethylene was calculated based on the total amount of carbon in acetylene converted into ethylene.

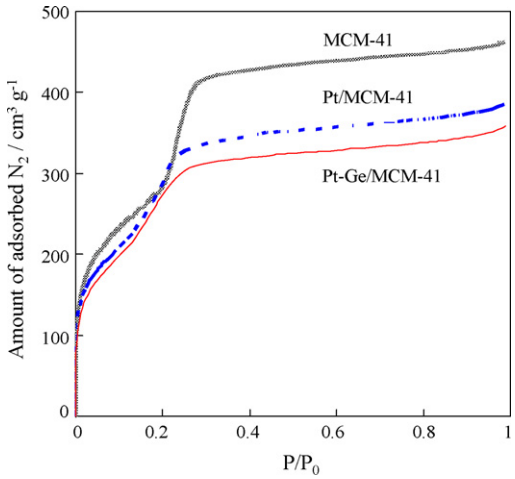

Fig. 1. N_2 adsorption isotherms on MCM-41 catalysts.

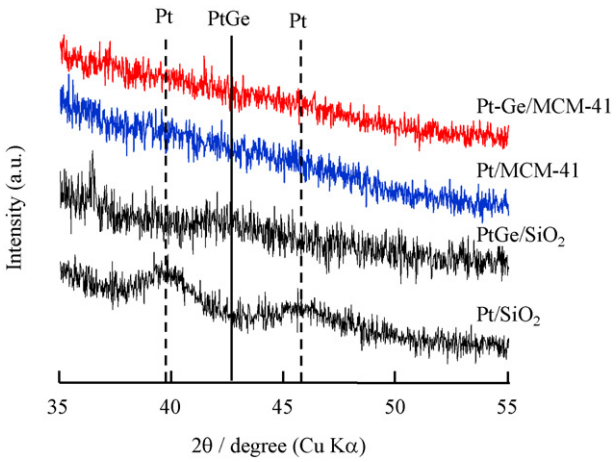

Fig. 3. XRD patterns of SiO_2- and MCM-41-supported catalysts.

3. Results and discussion

3.1. Characterization of Pt/MCM-41 and Pt-Ge/MCM-41 catalysts

The mesopore structure in MCM-41 is not so stable compared with the micropore structure in zeolites. Therefore, the structural characterizations were first carried out for the parent MCM-41 as well as Pt/MCM-41 and Pt-Ge/MCM-41. Fig. 1 shows the N_2 adsorption isotherms for these catalysts. Upon Pt loading of 0.70 wt%, the amount of N_2 adsorption decreased significantly, suggesting the partial collapse of mesopores or blockage of mesopores by Pt particles. In addition, the steep increase in N_2 uptake around $P/P_0 = 0.2$ became rather gradual, indicating the slight loss of structural regularity of mesopores. However, the subsequent loading of Ge (Pt/Ge atomic ratio of 1.3) did not affect the isotherm significantly. The pore volumes of MCM-41, Pt/MCM-41 and Pt-Ge/MCM-41 were estimated to be 0.72, 0.60 and 0.56 $cm^3\ g^{-1}$, respectively.

The MCM-41 structure was further studied by XRD as shown in Fig. 2. The parent MCM-41 showed a typical diffraction pattern of hexagonal structure. Pt/MCM-41 and Pt-Ge/MCM-41 showed a strong peak around $2\theta = 2^\circ$ by (1 0 0) diffraction though other peaks had lower intensity than those of MCM-41. The angle of the (1 0 0) peak was almost the same for all the catalysts. The pore diameter would not be affected by Pt and Ge loadings. Since the pore size of parent MCM-41 was calculated to be 2.6 nm from SAXS pattern [27], both Pt/MCM-41 and Pt-Ge/MCM-41 will have the pore diameter of about 2.6 nm.

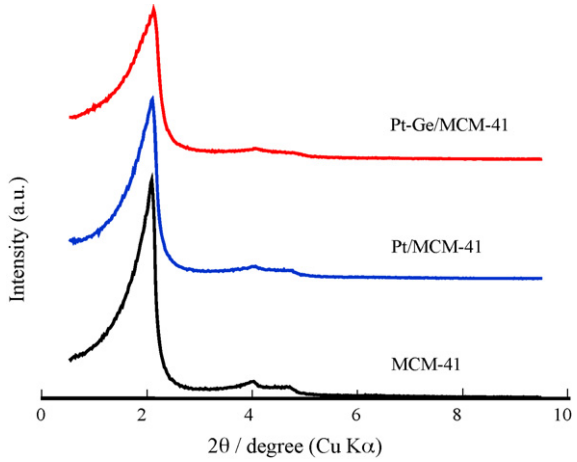

Fig. 2. XRD patterns of MCM-41 catalysts.

The nature of supported metals was then characterized. First, we measured XRD in the higher angle region as shown in Fig. 3, and compared the XRD pattern with those of silica-supported catalysts prepared by similar procedures to MCM-41-supported ones. Pt/SiO_2 gave two diffraction peaks attributed to metallic Pt at $2\theta = 39.8^\circ$ and 46.2°. The crystallite size was estimated to be 4 nm by Scherrer's equation. This was a little smaller than the average pore diameter (6 nm) of the silica gel used. On the other hand, $Pt\text{-}Ge/SiO_2$ gave a very broad peak around $2\theta = 43^\circ$ without appreciable peaks attributed to Pt metal. Because an IMC of PtGe (orthorhombic structure) gives the diffraction at 42.6°, small particles of PtGe would be formed through the CVD using $Ge(CH_3)_4$ onto Pt/SiO_2. Hereafter, we designate this catalyst as $PtGe/SiO_2$ though the peak width was too broad for the application of Scherrer's equation to estimate the PtGe crystallite diameter. Because Ge was introduced onto Pt/SiO_2, PtGe particles should have a little larger diameter than Pt particles in Pt/SiO_2. The broad peak would result from the coexistence of another intermetallic phase, Pt_3Ge_2 (41.9°). In the case of MCM-41-supported catalysts, however, the diffraction by metallic species could not be observed. Pt particles in Pt/MCM-41 will be very small, which implies that Pt particles are located inside the mesopores of MCM-41. The formation of intermetallic phases between Pt and Ge was not revealed for Pt-Ge/MCM-41, suggesting that the metal particles are also very small.

To obtain the information about the location of metal particles, we carried out TEM observations for $PtGe/SiO_2$ and Pt-Ge/MCM-41 (Fig. 4). The particle diameter was measured from the TEM images and its distribution is shown in Fig. 5. $PtGe/SiO_2$ consisted of metallic particles, probably PtGe, with diameters of 1–6 nm. It is clear that PtGe particles on SiO_2 are heterogeneous in their diameter. In contrast, Pt-Ge/MCM-41 consisted of small metallic particles with diameters around 1.5 nm, which was smaller than the pore diameter of the parent MCM-41 (2.6 nm). Though the ordered mesopores could not be clearly seen in the high magnification image (Fig. 4b), the high homogeneity in particle diameter smaller than the pore size and the absence of particles concentrated at the edge of MCM-41 crystallites both indicate that Pt-Ge particles are located inside the mesopores of MCM-41.

Amounts of adsorbed CO and H_2 were measured at 298 and 195 K, respectively, to know the dispersion and diameter of metal particles. As shown in Table 1, Pt/SiO_2 adsorbed CO in the amount of 1.7 mmol g-Pt^{-1}, which was twice as large as the amount of adsorbed H_2. Hydrogen is dissociatively adsorbed on the surface Pt atoms. The difference in the CO and H_2 uptakes will be explained

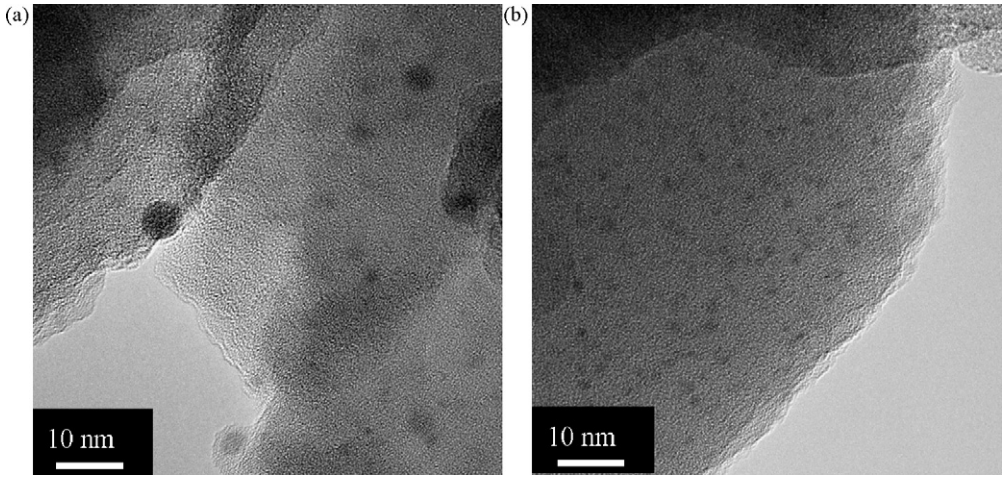

Fig. 4. TEM images of $PtGe/SiO_2$ (a) and Pt-Ge/MCM-41 (b).

Table 1
Characterization of catalysts.

Catalyst	Pt loading (wt%)	Pt/Ge atomic ratio	Amount of adsorbed CO (mmol g-Pt^{-1})	Amount of adsorbed H_2 (mmol g-Pt^{-1})
Pt/SiO_2	1.0	–	1.7	0.87
$PtGe/SiO_2$	1.0	0.80	0.46	0.45
Pt/MCM-41	0.70	–	3.1	3.8
Pt-Ge/MCM-41	0.70	1.3	1.3	1.7

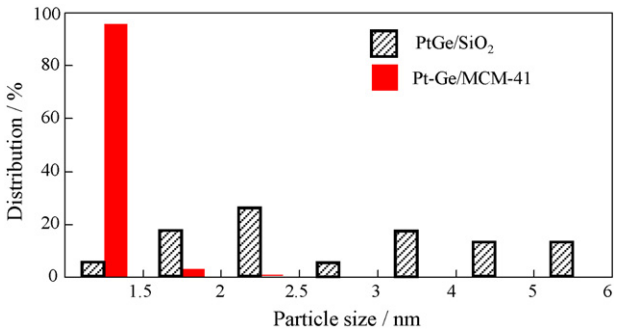

Fig. 5. Particle size distribution obtained from TEM images.

by the idea that both CO and hydrogen are adsorbed at on-top sites of Pt and that CO is adsorbed as linear species. The particle diameters calculated from these uptakes, by assuming that Pt atoms form truncated octahedron crystallites, are shown in Table 2 together with the crystallite diameter estimated by XRD and the average particle diameter obtained by TEM. In the case of Pt/SiO_2, the crystallite diameter and particle diameter obtained from these techniques gave almost the same value of 4 nm, indicating the measurements of the diameter should be fairly accurate. In the case of $PtGe/SiO_2$, CO uptake was almost the same as H_2 uptake. As mentioned below, a part of adsorbed CO may be too weakly retained on the surface of PtGe under flowing helium at 298 K. In any case a comparable amount of H_2 to that of CO was adsorbed on $PtGe/SiO_2$. This is a different result from that reported for Ni_3Sn/SiO_2 [28], on which the amount of adsorbed H_2 was less than one-tenth of that of adsorbed CO. The inhibiting effect of IMC formation on the H_2 adsorption was explained by the extension of atomic distance between adjacent Ni atoms by the incorporation of Sn atoms to form Ni_3Sn. The crystal structure of PtGe (orthorhombic) is totally different from that of Pt metal (cubic). However, the atomic distance between adjacent Pt atoms may not be extended so much through the IMC formation.

As shown in Table 1, the CO and H_2 uptakes on Pt/MCM-41 were larger than those on Pt/SiO_2, indicating the smaller Pt particle size on MCM-41 than that on SiO_2 as mentioned above. The H_2 uptake on Pt/MCM-41 was larger than the CO uptake. Physical adsorption of H_2 on MCM-41 may increase the uptake for MCM-41-supported catalysts. The contribution of physical adsorption will be discussed later. As shown in Table 2, the average particle diameter calculated from the CO uptake on Pt/MCM-41 was again smaller than the pore size of MCM-41. On Pt-Ge/MCM-41, the H_2 uptake was larger than the CO uptake, as in the case of Pt/MCM-41. This could be explained by the physical adsorption of H_2 as well as the weak CO adsorption. As shown in Table 2, TEM showed that the particle diameter of Pt-Ge catalysts was smaller than that of Pt catalysts both on SiO_2 and MCM-41 supports. Because Ge was introduced onto Pt/SiO_2 and Pt/MCM-41, it is not reasonable that the Ge incorporation decreased the particle diameter. The lower density of Pt-Ge particles may make their outline obscure in TEM images.

From the above results, we conclude that in Pt-Ge/MCM-41, Pt-Ge metallic particles are located inside the mesopores of MCM-41 having the particle diameter around 1.5 nm. Then we discuss on what kind of compound or its mixture exist as the Pt-Ge particles. IR spectra of adsorbed CO were measured to clarify the geometric and electronic nature of the Pt-Ge particles and Pt particles on MCM-41 and SiO_2. Fig. 6 shows the spectra obtained after CO adsorption

Table 2
Particle and crystallite sizes of supported metal.

Catalyst	Crystallite diameter by XRD (nm)	Average particle diameter (nm) determined by		
		TEM	CO adsorption	H_2 adsorption
Pt/SiO_2	4	4.8	4.0	3.9
$PtGe/SiO_2$	<4	4.0	n.d.[a]	n.d.[a]
Pt/MCM-41	–	1.8	2.0	n.d.
Pt-Ge/MCM-41	–	1.4	n.d.[a]	n.d.[a]

[a] Not determined.

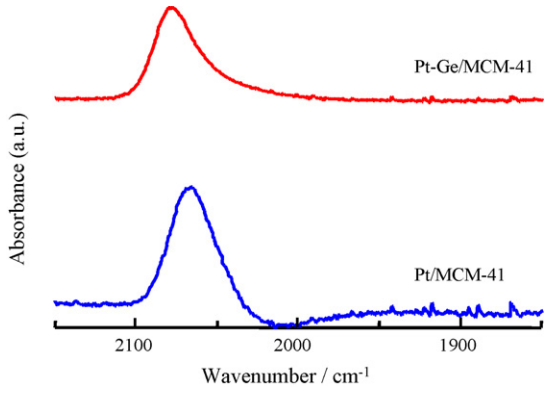

Fig. 6. IR spectra of CO adsorbed at 298 K.

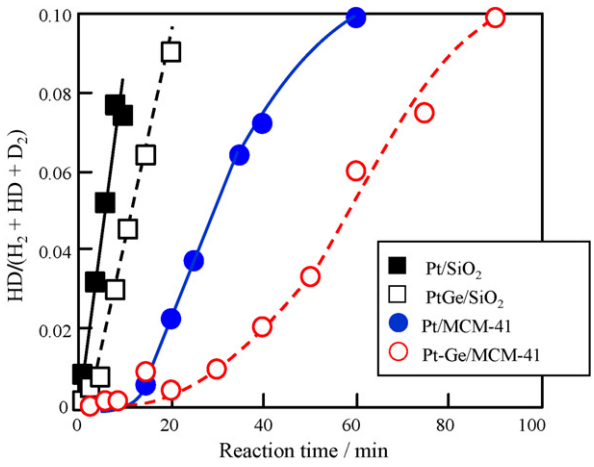

Fig. 8. H_2–D_2 equilibration at 77 K.

and the subsequent evacuation at 298 K. Pt/MCM-41 gave a strong absorption peak around 2070 cm^{-1} and a weak and broad band around 1920 cm^{-1}. The former will be attributed to the linear CO species and the latter to the bridging CO species. In contrast, Pt-Ge/MCM-41 did not gave the band of bridging species, whereas the linear species gave a strong peak at 2080 cm^{-1}. Similar disappearance of bridging CO species has been observed for supported IMC catalysts of Ni_3Sn_4/SiO_2 [28], Pt_3Co/SiO_2 [29], $PtCu/SiO_2$ [29] and Ni_3Ge/SiO_2 [22]. The formation of these IMCs extends the atomic distance of adjacent Ni or Pt atoms, which would hinder the formation of bridging CO species. In this study, the disappearance of bridging CO could be an evidence for the formation of IMC between Pt and Ge on MCM-41. We already mentioned that the surface Pt–Pt atomic distance is not extended so much through the formation of PtGe, resulting in the significant amount of H_2 adsorbed on PtGe. Therefore, the formation of bridging CO species would be highly sensitive to the surface Pt–Pt distance compared with the H_2 adsorption.

The peak position of linear CO species will be a measure of the electronic nature of the metal atoms at the adsorption site. Fig. 7 shows the relation between the peak position of the linear CO band and the evacuation temperature before the spectrum acquisition for Pt and Pt-Ge supported on MCM-41 and SiO_2. The peak top shifted to lower wavenumber with increasing evacuation temperature on all the catalysts, indicating the decrease in repulsive interaction between adjacent CO species because of the decrease in surface coverage. At higher evacuation temperatures, the peak position should reflect the electronic state of Pt atoms bound to CO. Though the peak position was not steady for all the catalysts at higher temperatures, the electronic state of Pt might be discussed based on the peak position at the highest temperature for each catalyst. Above this temperature, the CO coverage was too low to detect the IR band. On SiO_2, Pt gave the peak at 2046 cm^{-1}, whereas PtGe gave it at 2055 cm^{-1}. The higher wavenumber on PtGe indicates that CO adsorbs on PtGe more weakly than on Pt. This would correspond to the lower electron density of Pt atoms on PtGe particles, that is, the decrease in the back donation from Pt to CO. A similar peak shift has been observed for Ni_3Ge/SiO_2 and Ni/SiO_2, where CO adsorbed on Ni_3Ge and Ni gave the peak at 2055 and 2025 cm^{-1}, respectively. The change in the electronic state of Pt in PtGe would be a proof of the formation of IMC. In the cases of MCM-41-supported catalysts, a similar difference in peak position was observed, that is, 2064 cm^{-1} on Pt-Ge and 2050 cm^{-1} on Pt. This could be another proof of the formation of IMC, probably PtGe, inside the pores of MCM-41. Fig. 7 further shows that MCM-41-supported catalysts gave slightly higher wavenumbers than SiO_2-supported ones. This might be caused by the interaction between the adsorbed CO and the pore wall of MCM-41.

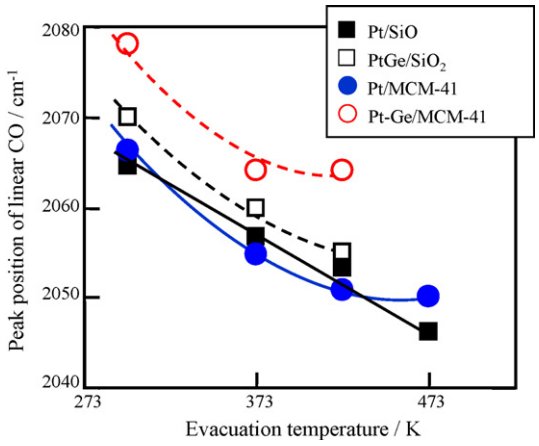

Fig. 7. Effect of evacuation temperature on IR peak position of linear CO species.

3.2. Catalytic reactions on Pt/MCM-41 and Pt-Ge/MCM-41 catalysts

The catalytic properties of Pt-Ge particles in MCM-41 was first studied for H_2–D_2 equilibration in a closed circulation system to clarify the ability to dissociate hydrogen molecules. Fig. 8shows the change in the fraction of HD in hydrogen molecules with reaction time obtained at 77 K. $PtGe/SiO_2$ gave a slightly lower HD formation rate than Pt/SiO_2. As shown in Table 2, the metal particle sizes of these catalysts were almost the same. Therefore, the specific activity per surface metal atom of $PtGe/SiO_2$ would be in the same order of magnitude as that of Pt/SiO_2. We have studied the catalytic activity of IMCs between a transition metal and a typical element for H_2–D_2 equilibration and found two different results. In the case of CoGe [2], Ni_3Sn, Ni_3Sn_2, Ni_3Sn_4 [3], Pt_3Ge, Pt_2Ge and PtGe [6], they exhibited much lower activity than the corresponding pure transition metal, Co, Ni and Pt catalyst, respectively. For example, unsupported Ni powder catalyzed the HD formation in an observable rate at 373 K, whereas Ni_3Sn powder required the reaction temperature of 523 K to catalyze the reaction in a comparable rate [3]. On the other hand, turnover frequencies (TOFs) for HD formation on Ni_3Ge/SiO_2 and Ni/SiO_2 were 0.062 and 0.076 s^{-1}, respectively, under the same reaction conditions [22], indicating the comparable activity of Ni_3Ge to that of Ni. $PtGe/SiO_2$ in this study would correspond to the latter case. However, as we reported previously [6], on unsupported PtGe, the H_2–D_2 equilibration did not occur in an appreciable rate at 298 K, whereas on Pt powder, the

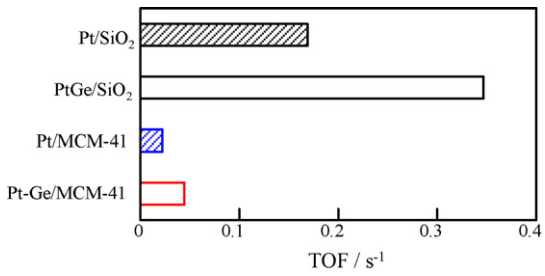

Fig. 9. TOF for H_2–D_2 equilibration.

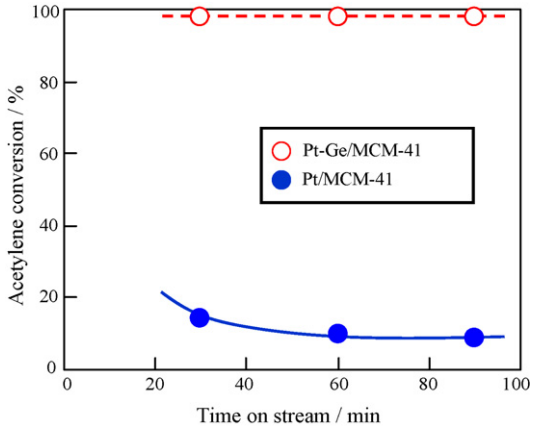

Fig. 11. Change in conversion with time on stream for the hydrogenation of acetylene at 573 K.

reaction reached the equilibrium within 30 min at the same temperature. On both catalysts, the metal particles had the same size of 50–90 μm. These results indicate that PtGe has much lower specific activity than Pt. It is concluded that PtGe is much less active than Pt when unsupported catalysts are used but that it is comparably active to Pt when they are finely dispersed on SiO_2. The contradictory results for PtGe might be explained by the difference in the particle size. The unsupported PtGe has the particle size of 50–90 μm, whereas PtGe/SiO_2 contains PtGe particles with the diameter of ca. 1–6 nm. Assuming that the Pt particles on SiO_2 have a similar specific activity to the unsupported ones, the nano-size effect could result in the high specific activity of supported PtGe as in the case of gold nano particles [30].

As shown in Fig. 8, Pt/MCM-41 and Pt-Ge/MCM-41 catalysts gave slightly lower HD formation rates than the SiO_2-supported counterparts. Table 2 shows that the metal particle size in the MCM-41-supported catalysts was smaller than that in the SiO_2-supported ones. These results indicate that the MCM-41-supported catalysts have the lower specific activity than the SiO_2-supported ones. Therefore, we considered the steric hindrance for the diffusion of hydrogen molecules inside the mesopores of MCM-41. Since we carried out the reaction at the very low temperature of 77 K, the physical adsorption of hydrogen molecules will occur on the surface of MCM-41 as well as on metal particles. Such adsorbed hydrogen molecules could narrow the space between the metal particle and the inner wall of MCM-41, which will hinder the diffusion of hydrogen molecules. In addition to the low activity, Pt/MCM-41 and Pt-Ge/MCM-41 showed the induction period of 10–15 min before the reaction took place. The steric hindrance mentioned above may retard the diffusion of HD molecules produced beyond the metal particles through the narrow space, which could result in the induction period. In other words, the induction period observed for MCM-41-supported catalysts would be another proof of the existence of Pt or Pt-Ge particles inside the mesopores.

TOF for HD formation was calculated based on the slope of Fig. 8 and the amount of adsorbed CO as the number of surface Pt atoms. Fig. 9 clearly shows that both on SiO_2 and on MCM-41, Pt-Ge catalysts showed higher TOF than Pt catalysts, though the adsorption of CO on PtGe would be weak. As mentioned above, the absence of bridging CO species suggests that the atomic distance between adjacent Pt atoms in PtGe is slightly larger than that in pure Pt. The surface Pt–Pt distance in PtGe may be appropriate for the dissociative adsorption of hydrogen molecules, which could induce the higher TOF of PtGe catalysts for HD formation.

The catalytic properties of Pt-Ge/MCM-41 were further studied for the hydrogenation of acetylene using the continuous flow reaction system. Fig. 10 shows the relation between ethylene selectivity and acetylene conversion obtained at various times on stream. At 473 K (a), Pt-Ge catalysts gave much higher selectivity than Pt catalysts though the conversion on the latter was very high. To compare the selectivity at the comparably high conversion, the reaction was carried out at 573 K (b). Pt-Ge catalysts still gave high selectivity to ethylene with the conversion close to 100%. Pt catalysts gave high selectivity but the conversion decreased to less than 20%, indicating the deactivation probably by the accumulation of polymerized species. Fig. 11 shows the change in acetylene conversion with time on stream at the reaction temperature of 573 K. From Fig. 10(a), the higher conversion was expected for Pt/MCM-41. However, the conversion at 30 min on stream was lower than 20%. The fast deactivation of Pt/MCM-41 should have occurred during the initial 30 min

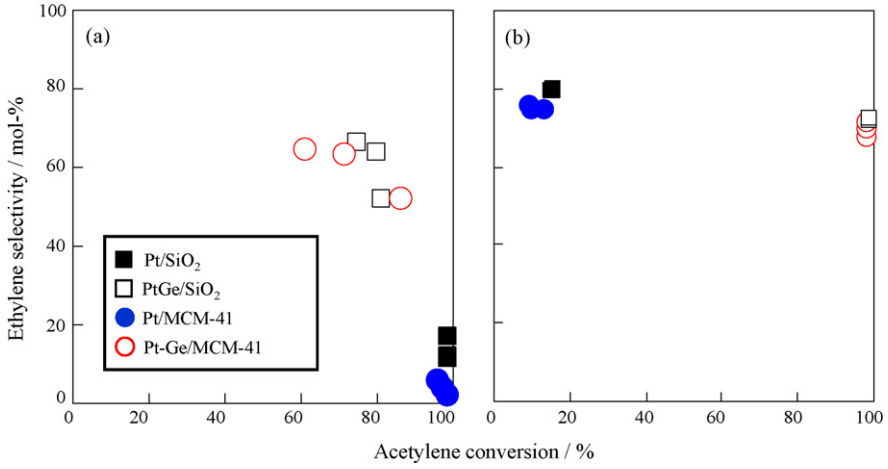

Fig. 10. Selectivity to ethylene in the hydrogenation of acetylene at 473 K (a) and 573 K (b).

on stream. The deactivation of metal catalysts in the acetylene hydrogenation has been reported to be caused by the green oil formation on the surface. The higher and more stable conversion on Pt-Ge/MCM-41 would indicate the superiority of PtGe intermetallic compound for the reaction of acetylene. In addition, from the selectivity at the conversions close to 100% shown in Fig. 10(b), it is clear that PtGe supported both on SiO_2 and MCM-41 is highly selective for the partial hydrogenation of acetylene into ethylene. The high selectivity to ethylene in the acetylene hydrogenation is the typical catalytic property found for some IMC catalysts, CoGe [2], Ni_3Sn_2 [3], NiZn [4], PdGa [5], Ni_3Ge/MCM-41 [22] and Pd_3Bi/SiO_2 [31].

4. Conclusions

Fine and homogeneous particles of Pt-Ge IMC useful to investigate the catalytic properties of Pt-Ge IMC are prepared by using the mesopores of MCM-41 as a kind of template.

Through the CVD treatment with $Ge(CH_3)_4$ onto Pt/MCM-41, fine particles of Pt-Ge IMC, probably PtGe, are formed inside the mesopores of MCM-41. The particle size is within the narrow range around 1.5 nm because the mesopores of MCM-41 with diameter of 2.6 nm prevent the PtGe particles from sintering into large particles. The catalytic activity of PtGe/MCM-41 for H_2–D_2 equilibration is comparable to that of Pt/MCM-41, though that of unsupported PtGe powder with the diameters of 50–90 μm is much lower than that of Pt powder with similar diameters. The comparable activity of PtGe fine particles to Pt for the H_2 dissociation may be explained by a kind of nano-size effect. PtGe inside the mesopores of MCM-41 suffers from the diffusion limitation generated at the narrow space between the PtGe particles and the mesopore wall. PtGe particles are highly selective for the formation of ethylene in the hydrogenation of acetylene at high conversion compared with Pt particles both on silica gel and MCM-41 supports.

Acknowledgements

This work was partly supported by Grant-in-Aid for Creative Scientific Research from the Ministry of Education, Science and Culture, Japan. We thank Professor Asai for the SAXS measurement, and Mr. Genseki and Center for Advanced Materials Analysis, Tokyo Institute of Technology for the TEM measurement.

References

[1] T. Komatsu, A. Onda, Catal. Surv. Asia 12 (2008) 6–15.
[2] T. Komatsu, M. Fukui, T. Yashima, Stud. Surf. Sci. Catal. 101 (1996) 1095–1104.
[3] A. Onda, T. Komatsu, T. Yashima, Phys. Chem. Chem. Phys. 2 (2000) 2999–3005.
[4] F. Studt, F. Abild-Pedersen, T. Bligaard, R.Z. Sørensen, C.H. Christensen, J.K. Nørskov, Science 320 (2008) 1320–1322.
[5] K. Kovnir, M. Armbrüster, D. Teschner, T.V. Venkov, F.C. Jentoft, A. Knop-Gericke, Y. Grin, R. Schlögl, Sci. Technol. Adv. Mater. 8 (2007) 420–427.
[6] T. Komatsu, S. Hyodo, T. Yashima, J. Phys. Chem. B 101 (1997) 5565–5572.
[7] T. Komatsu, D. Satoh, A. Onda, Chem. Commun. (2001) 1080–1081.
[8] T. Komatsu, T. Uezono, J. Jpn. Pet. Inst. 48 (2005) 76–83.
[9] A.P. Tsai, S. Kameoka, Y. Ishii, J. Phys. Soc. Jpn. 73 (2004) 3270–3273.
[10] R. Bacaud, P. Bussiere, F. Figueras, J. Catal. 69 (1981) 399–409.
[11] N. Iwasa, S. Masuda, N. Ogawa, N. Takezawa, Appl. Catal. A: Gen. 125 (1995) 145–157.
[12] J. Llorca, P.R. de la Piscina, J.L.G. Fierro, J. Sales, N. Homs, J. Catal. 156 (1995) 139–146.
[13] A. Onda, T. Komatsu, T. Yashima, J. Catal. 201 (2001) 13–21.
[14] T. Komatsu, Y. Fukui, Appl. Catal. A: Gen. 279 (2005) 173–180.
[15] J. Ruiz-Martínez, Y. Fukui, T. Komatsu, A. Sepulveda-Escribano, J. Catal. 260 (2008) 150–156.
[16] T. Komatsu, K. Inaba, T. Uezono, A. Onda, T. Yashima, Appl. Catal. A: Gen. 251 (2003) 315–326.
[17] T. Komatsu, H. Ikenaga, J. Catal. 241 (2006) 426–434.
[18] J.L. Carter, J.A. Cusumano, J.H. Sinfelt, J. Phys. Chem. 70 (1966) 2257–2263.
[19] M. Boudart, A.W. Aldag, L.D. Ptak, J.E. Benton, J. Catal. 11 (1968) 35–45.
[20] J.P. Brunelle, A. Sugier, J.F. Le Page, J. Catal. 43 (1976) 273–291.
[21] D.J.C. Yates, J.H. Sinfelt, J. Catal. 8 (1967) 348–358.
[22] T. Komatsu, T. Kishi, T. Gorai, J. Catal. 259 (2008) 174–182.
[23] M. Iwamoto, Y. Tanaka, Catal. Surv. Jpn. 5 (2001) 25–36.
[24] T. Abe, T. Tachibana, T. Uematsu, M. Iwamoto, J. Chem. Soc. Chem. Commun. (1995) 1617–1618.
[25] K. Chao, Y. Chang, Y. Chen, A. Lo, T. Phan, J. Phys. Chem. B 110 (2004) 1638–1646.
[26] S. Freni, S. Cavallaro, N. Mondello, L. Spadaro, F. Frusteri, J. Power Souces 108 (2002) 53–57.
[27] Y. Tominaga, S. Igawa, S. Asai, M. Sumita, Electrochim. Acta 50 (2005) 3949–3954.
[28] A. Onda, T. Komatsu, T. Yashima, J. Catal. 221 (2003) 378–385.
[29] T. Komatsu, A. Tamura, J. Catal. 258 (2008) 306–314.
[30] M. Haruta, N. Yamada, T. Kobayashi, S. Iijima, J. Catal. 115 (1989) 301–309.
[31] T. Komatsu, T. Gorai, Abst. 14th Intern. Congr. Catal. OB31 (Seoul), 2008, p. 68.